Remedy Open Access

Research Article
Published: 23 Nov, 2016

Candidate Alpha-emitting Radionuclides for Tumor Vascular Disruption Therapy

Bevelacqua JJ*

Bevelacqua Resources, USA

Abstract

Microspheres loaded with alpha-emitting radionuclides are an alternative to using ^{90}Y to facilitate tumor vascular disruption. Targeting a tumor's vasculature can be accomplished while minimizing the absorbed dose to healthy tissue by utilizing alpha-emitting radionuclides having limited beta-gamma emissions.

Keywords: Alpha loaded microspheres; Targeted alpha therapy; Tumor vascular disruption; Radiotherapy; Absorbed Dose

Introduction

A significant issue associated with radiotherapy procedures is that agents delivering an ionizing radiation dose to tumor cells also irradiate healthy tissue [1-6]. The irradiation of healthy tissue affects the patient's quality of life and leads to short-term as well as long-term detriments. Although the short-term detriment varies with the specific therapy approach, it is illustrated with prostate cancer radiotherapy methods. The short-term effects can include incontinence and erectile dysfunction that affects the patient's recovery and subsequent quality of life [7]. Long-term effects of radiotherapy can include secondary cancers and cardiovascular disease [8]. For these reasons, it is important to continue to investigate alternative radiotherapy approaches that deliver dose selectively to the target tissue and minimize dose to healthy tissue.

This paper considers a vascular disruption approach that has the potential to significantly minimize the dose to healthy tissue. The technique utilizes an enhancement of the ^{90}Y microsphere protocol that has been successfully utilized to treat liver cancers by disrupting the tumor's vasculature. A number of authors [9,10] have proposed a microsphere therapy approach that prevents the development of the tumor's vasculature. Vascular disruption methods include both chemotherapy [11,12] as well as radiotherapy [12-23]. Radiotherapy vascular disruption techniques have been extensively applied to liver cancers [12-17] utilizing ^{90}Y microspheres. Other radionuclides (e.g., ^{32}P) have been less thoroughly investigated and radiation types other than high-energy beta particles have not been systematically investigated [12].

This paper focuses on alpha–emitting radionuclides with the goal of depositing energy within 100 μm of the microsphere. This degree of localization can be achieved using alpha-emitting radionuclides with minimal beta and gamma emissions.

Materials and Methods

The proposed microsphere approach is currently limited to a theoretical treatment. This is expected since this initial investigation determines the appropriate alpha-emitting radionuclides and associated energies, and ascertains the viability of the technique. The present work determines these characteristics, which is the first step in developing the proposed microsphere vascular disruption therapy approach. Subsequent steps involve the detailed design of the microsphere in terms of the specific materials of construction, optimum size, and radionuclide distribution. Experimental work would follow the completion of the aforementioned tasks and construction of the microspheres.

This situation is similar to the development of an antiproton therapy modality [22,23]. Theoretical calculations were the first step in establishing the feasibility of antiproton therapy. These calculations required several years to establish the appropriate parameters for an experimental approach.

Tumor vasculature

One of the most striking characteristics of solid tumors is their vasculature. In normal tissues, the

OPEN ACCESS

Correspondence:
Bevelacqua JJ, Bevelacqua Resources, 343 Adair Drive, Richland, WA 99352 USA,
E-mail: bevelresou@aol.com

Received Date: *18 Sep 2016*
Accepted Date: *21 Nov 2016*
Published Date: *23 Nov 2016*

Citation:
Bevelacqua JJ. Candidate Alpha-emitting Radionuclides for Tumor Vascular Disruption Therapy. Remed Open Access. 2016; 1: 1027.

Table 1: Characteristics of Various Blood Vessel Types[a].

Blood Vessel Type	Wall Thickness	Lumen Diameter
Aorta	2 mm	25 mm
Artery	1 mm	4 mm
Arteriole	20 μm	30 μm
Capillary	1 μm	8 μm
Venule	2 μm	20 μm
Vein	0.5 mm	5 mm
Vena Cava	1.5 mm	30 mm

[a]Barrett *et al*. [24].

vasculature structure is arranged to provide optimum nourishment.

However, growing tumors have a chaotic vasculature that is not fully developed or adequate to optimally nourish the tumor cells [11]. Given this condition, the tumor's vasculature can be disrupted with an appropriate agent.

Common defects in a tumor's vascular structure include vessels that are dilated and have elongated shapes, blind ends, bulges, leaky sprouts, and abrupt changes in diameters [11]. Accordingly, blood flow in these vessels is sluggish and irregular and results in hypoxic areas that are characteristic of solid tumors. The lack of oxygen provides a degree of radioresistance to tumor cells when compared with oxygenated cells. Since a tumor's growth is dependent on sufficient nourishment, its viability is affected by disrupting the blood supply. In principle, eliminating a tumor's blood supply offers an alternative means to facilitate or supplement its destruction.

Current radiological efforts

Radiological efforts at tumor vascular disruption have focused on ^{90}Y. ^{90}Y was a logical choice for anti-angiogenic therapy since the dose to destroy a tumor is ≥70 Gy, and this is easily achieved using ^{90}Y. However, the ^{90}Y beta particles have significant range and extend well beyond the vascular target. The maximum beta energy of 2.27 MeV has a range in tissue of about 1.1 cm, which delivers considerable absorbed dose beyond the target vascular structure. ^{90}Y bremsstrahlung provides additional dose to healthy tissue. The properties of ^{90}Y microspheres used in therapy applications are summarized by Kennedy et *al*. [16].

Medical reviews suggest the ^{90}Y approach is a safe and effective therapy method for selected patients. However, a number of negative features are associated with ^{90}Y microsphere therapy [16]. First, ^{90}Y bremsstrahlung affects healthy tissue well beyond the vasculature. Second, resin microspheres may have trace ^{90}Y on their surface, which can be excreted via urine and deliver absorbed dose to healthy tissues in this excretion pathway. Third, for glass microspheres, 150 Gy is the dose delivered to the target tissue. The recommended cumulative lung dose should be maintained below 30 Gy to prevent radiation pneumonitis. Fourth, ^{90}Y microsphere patients can experience short-term abdominal pain, fatigue, and nausea. Fifth, radioembolization to nontarget tissues can cause other acute damage that result in gastrointestinal ulceration, pancreatitis, and radiation pneumonitis. Late effects can include radiation induced liver disease. These negative features motivate an investigation of alpha-emitting microspheres to minimize the dose to healthy tissue.

Theoretical approach

Table 1 summarizes wall thickness for a variety of human blood vessel types [24], and some of these could service a developing tumor [11]. A review of the literature indicates developing tumor vessel wall sizes are typically less than 100 μm [11]. This wall size includes arterioles, which is the assumed base case for the discussion presented in this paper.

Absorbed dose computational model

The absorbed dose delivered to the target vasculature is evaluated using the methodology outlined in Refs. 1-6. This methodology includes methods to calculate charged particle and photon doses.

Charged particle absorbed dose: For a tissue volume irradiated by ions of a given energy, the absorbed dose (D) as a function of penetration distance x into tissue is [1-6,25]:

$$D(x) = \frac{1}{\rho}\left(-\frac{dE}{dx}\right)\Phi(x) \qquad (1)$$

where ρ is the density of the material attenuating the ion, -dE/dx is the stopping power, and Φ(x) is the ion fluence at the location of interest based on the microsphere activity. The particle fluence varies with tissue penetration depth according to the relationship:

$$\Phi(x) = \Phi(0)e^{-\Sigma x} \qquad (2)$$

where Φ(0) is the entrance fluence and Σ is the macroscopic reaction cross-section. Ion stopping powers are determined using Bethe's formulation [26], the energy dependent cross-sections are obtained from Shen et al. parameterization [27] or models [1-6].

Photon absorbed dose: The photon absorbed dose is derived from the standard point source relationship [4-6]

$$D = \frac{S}{4\pi r^2}\frac{\mu_{en}}{\rho}E\ B(\mu x)e^{-\mu x} \qquad (3)$$

where S is the total number of photons that irradiates the arteriole wall, r is the distance from the microsphere, μ_{en}/ρ is the mass-energy absorption coefficient, E is the photon energy, B is a buildup factor, and μ is the attenuation coefficient.

The photon absorbed dose contribution was calculated using the ISO-PC computer code [28].

General alpha particle deposition profile: Figure 1 illustrates the results of calculations for the dose delivered by alpha particles to vascular depths up to 100 μm using a total fluence of 5.0 x 10^8 ^{4}He ions/cm^2. Alpha energies in the range of 3–8 MeV are presented and these energies are achieved by many candidate alpha-emitting

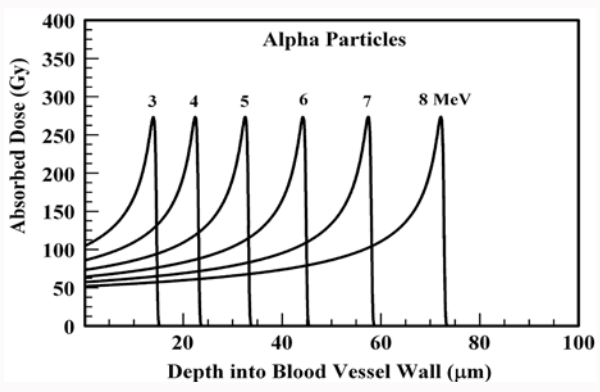

Figure 1: Absorbed dose profiles for 3.0-8.0 MeV ^{4}He ions in water. The absorbed dose curves peak at a greater depth with increasing ^{4}He ion energy. The total fluence for all energies is 5.0x10^8 ^{4}He ions/cm^2.

Table 2: Alpha-Emitting Radionuclides for Potential Vascular Disruption Applications[a,b].

Nuclide	$T_{1/2}$	Radiation Type / Energy (MeV)		
		Alpha	Beta[c]	Gamma
^{149}Tb	4.12 h	3.969	1.8	0.1650 0.3522
^{206}Po	8.8 d	5.223	---	0.2864 0.5113 0.8074 1.0323
^{211}At[d]	7.21 h	5.868	---	0.6696 (w) 0.6870 (w)
^{212}Bi	1.009 h	6.051	2.251	0.0399 0.7273
^{213}Bi	45.6 min	5.55 (w) 5.87	1.02 1.42	0.3237 (w) 0.4405
^{222}Rn[e]	3.8235 d	5.4895	---	0.510 (w)
^{223}Ra	11.435 d	5.607 5.7164	---	0.1542 0.2694 0.3239
^{224}Ra	3.63 d	5.449 5.6855	---	0.24099
^{225}Ac	10.0 d	5.731 5.793 5.829	---	0.0998
^{227}Th	18.68 d	5.757 5.978 6.038	---	0.0502 0.2360
^{230}U	20.8 d	5.818 5.888	---	0.0722 (w) 0.1542 0.2304

[a]Baum et al [30].
[b]Weak (w) transition with a yield <1%.
[c]Maximum beta or positron energy.
[d]See Table 3 for daughter radiation types and energies.
[e]See Table 4 for daughter radiation types and energies.

radionuclides. Relative biological effectiveness values are addressed in subsequent discussion [29].

Alpha particles with energies below 3 MeV will not penetrate the arteriole wall. The arteriole wall can be disrupted with minimal dose to surrounding tissue for alpha particles in the 4–5 MeV energy range. This energy range is obtained by numerous alpha-emitting radionuclides. The results of Figure 1 suggest that alpha emitting radionuclides could produce an alternative to the use of ^{90}Y in microspheres to disrupt a tumor's vascular structure.

Candidate alpha emitting radionuclides

A number of alpha-emitting radionuclides are currently available for potential therapeutic application including ^{149}Tb, ^{211}At, ^{212}Bi, ^{213}Bi, ^{223}Ra, ^{225}Ac, and ^{227}Th [6,30]. These radionuclides are useful in treating macroscopic tumors, but are only useful in a vascular disruption approach if the associated beta-gamma emissions are weak. Any significant beta or gamma energy from the candidate radionuclide or its daughters irradiates healthy tissue outside the target vascular volume.

Candidate alpha-emitting radionuclides with their associated half-lives and other radiation emissions are summarized in Table 2. These radionuclides are evaluated for their applicability to vascular disruption in subsequent discussion. Other radionuclides were addressed in Refs. 4-6.

Of the radionuclides listed in Table 2, only ^{221}At and ^{222}Rn have the potential for targeted vascular disruption. These are the only evaluated radionuclides that have alpha emissions with weak emissions of other radiation types. Other radionuclides considered in Table 2 will deliver absorbed dose beyond the vascular target regions of 100 μm.

General microsphere characteristics

Candidate microspheres are assumed to be loaded with primarily alpha-emitting radionuclides. Desirable characteristics for the radionuclide and candidate microsphere to facilitate tumor blood vessel disruption include the (1) nuclide should have a short effective half-life, (2) any emitted photon and beta radiation should be weak, (3) absorbed dose to the vascular wall should be at least 100 Gy, (4) dose delivered to healthy tissue should be minimized, (5) microsphere has the capability to preferentially attach to the wall of an arteriole supplying blood to the tumor, and (6) candidate radionuclide is chemically compatible with a microsphere that can be removed at a prescribed time from the body.

Although these characteristics provide a basis for the calculations presented in this paper, they have not been optimized to produce a viable alternative to the ^{90}Y microsphere approach.

However, they provide an initial set of reasonable parameters to determine the characteristics of a replacement microsphere.

Selection of radionuclide for vascular disruption

As noted in Section 2.5, ^{211}At and ^{222}Rn are possible radionuclides for use in vascular disruption. However, their daughter radiation must be evaluated to ensure that minimal absorbed dose is delivered to healthy tissue. The decay schemes of ^{211}At and ^{222}Rn are illustrated in Equations 4 and 5, respectively. The radiation emissions of ^{211}At (^{222}Rn) are provided in Table 3 [4].

$$^{211}At \xrightarrow{EC\,58\%} {}^{211}Po \xrightarrow{\alpha} {}^{207}Pb$$
$$\xrightarrow{\alpha\,42\%} {}^{207}Bi \xrightarrow{\beta^+} {}^{207}Pb \quad (4)$$

$$^{222}Rn \xrightarrow{\alpha} {}^{218}Po \xrightarrow{\alpha} {}^{214}Pb \xrightarrow{\beta^-} {}^{214}Bi \xrightarrow{\beta^-} {}^{214}Po \xrightarrow{\alpha} {}^{210}Pb \xrightarrow{\beta^-}$$
$$^{210}Bi \xrightarrow{\beta^-} {}^{210}Po \xrightarrow{\alpha} {}^{206}Pb \quad (5)$$

As noted in Table 3, ^{221}At has associated photon radiation derived by its ^{211}Po and ^{207}Bi daughters which deliver dose outside the target volume. In a similar manner, ^{222}Rn daughters have beta and gamma radiation types that deliver significant absorbed dose well beyond the arteriole wall. Accordingly, it is not an optimum radionuclide to deposit dose preferentially within the vascular wall. However, an examination of the ^{222}Rn decay chain suggests that ^{210}Po has the desired characteristics for vascular disruption without significantly irradiating healthy tissue. In particular, its 5.3 MeV alpha particle has sufficient energy to irradiate the arteriole wall while limiting absorbed dose beyond the target tissue. In addition, the weak 803 keV photon radiation with a yield of <1.0 x 10^{-3}% delivers minimal dose beyond the target tissue. Although its physical half-life is 138 days, a much shorter effective half-life can be achieved through careful design (See Section 3.3).

Table 3: ^{211}At and Its Daughters[a,b].

Nuclide	$T_{1/2}$	Radiation Type / Energy (MeV)		
		Alpha	Beta[c]	Gamma
^{211}At	7.21 h	5.868	---	0.6696 (w) 0.6870 (w)
^{211}Po	0.516 s	7.451	---	0.5692 (w) 0.8972
^{207}Bi	32 y	---	(w)	0.5697 1.0637
^{207}Pb	Stable	--	---	---

[a]Baum et al. [30].
[b]Weak (w) transition with a yield <1%.
[c]Maximum positron energy.

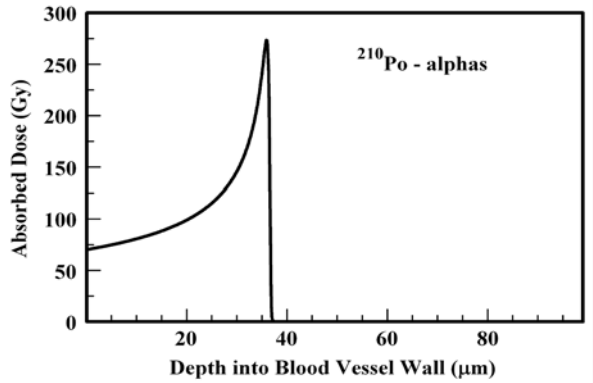

Figure 2: Absorbed dose profile for ^{210}Po alpha particles in a water medium. The absorbed dose is delivered by 0.3 Bq of ^{210}Po uniformly deposited within a 1 μm diameter microsphere following the total decay of the radioactive material.

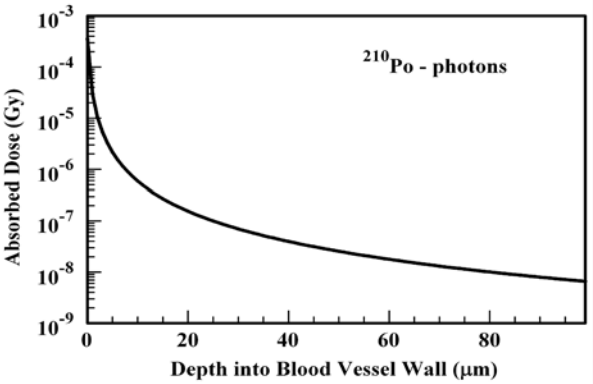

Figure 3: Absorbed dose profile for ^{210}Po photons in a water medium. The absorbed dose is delivered by 0.3 Bq of ^{210}Po uniformly deposited within a 1 μm diameter microsphere following the total decay of the radioactive material.

Base case microsphere design

The selected microsphere is loaded with ^{210}Po with an activity of 0.3 Bq that is uniformly distributed in a 1 μm diameter sphere. The sphere is comprised of a ^{12}C matrix with a density of 2.0 g/cm^3. The basis for the 0.3 Bq activity is provided in subsequent discussion.

Dose calculations are based on a single microsphere. Actual treatment protocols will entail a collection of these spheres with the number determined by the target cancer and its stage of development.

Relative biological effectiveness

The absorbed dose is often modified by the relative biological effectiveness (RBE) to account for the cell killing efficiency of a given radiation type. An RBE is usually defined as the ratio of a dose of reference energy photons to a dose of another radiation type that produces the same biological effect as the photons. Although the RBE is a relatively simple concept, its therapy application is complex [29]. This complexity arises because the RBE depends on the radiation type and its energy, the delivered absorbed dose, the delivery method, and the cell and tissue type that is irradiated. Given these uncertainties and the current stage of ^{210}Po microsphere development, no RBE is applied to the absorbed doses. Since the anticipated RBE values for alpha particles will be greater than unity, the absorbed dose for vascular disruption provided in this paper represents a lower bound of the performance of the ^{210}Po microsphere approach.

Results and Discussion

An activity of 0.3 Bq of ^{210}Po is sufficient to deliver an absorbed dose of about 100 Gy to the arteriole wall. No attempt was made to provide a more exact activity since the design has yet to be refined and must consider insertion and removal methods, fabrication details, and appropriate relative biological effectiveness values for the alpha and gamma ^{210}Po radiation types.

In performing the absorbed dose calculations, the ^{210}Po microsphere is assumed to reside at the inner arteriole wall. The results of the alpha and gamma contributions to the absorbed dose for blood vessel wall thickness values ≤100 μm from a ^{210}Po loaded microsphere are summarized in Figures 2 and 3, respectively. The gamma absorbed dose is significantly less than the alpha absorbed dose. Therefore, Figure 2 also represents the total absorbed dose delivered by the candidate ^{210}Po microsphere. Water is assumed to be the medium comprising the vessel wall which is a reasonable tissue surrogate for initial calculations [1-6,25].

Dose localization within the tumor vasculature is quite good with the peak dose delivered at 35.9 μm. At the Bragg peak, the ratio of alpha to gamma dose is 1.7 x 10^{10}. Beyond 37 μm, less than 0.1 μGy is delivered by the ^{210}Po photons. Although the ^{210}Po microsphere has good dose localization, its 138 d half-life is larger than currently used radionuclides ^{32}P (14.28 d) and ^{90}Y (2.669 d) [30].

Dose dependence on residence time

The results of the previous section are based on the dose delivered by the total decay of all microsphere activity. In view of the 138 d ^{210}Po half-life, it will be desirable to remove the microsphere before all activity has decayed.

The delivered dose rate as a function of time is given by the relationship:

$$\dot{D}(t) = \dot{D}(0)e^{-\lambda t} \qquad (6)$$

where λ is the ^{210}Po physical decay constant. The total delivered dose to the vascular wall during the residence time T is obtained by integrating the Equation 6:

$$D(T) = \frac{\dot{D}(0)}{\lambda}\left(1-e^{-\lambda T}\right) = D(\infty)\left(1-e^{-\lambda T}\right) \qquad (7)$$

Since the activity is proportional to the delivered dose, early removal of the microsphere at residence time T requires an increase in the initial activity loading by a factor F which is the ratio of D(∞)/D(T):

$$F = \frac{1}{\left(1-e^{-\lambda T}\right)} \qquad (8)$$

This activity increase delivers the required dose to disrupt the tumor's vasculature. For example, an activity of about 2 Bq (0.3 Bq x 7.19) is the requisite ^{210}Po activity loading to produce the doses summarized in Figures 2 and 3 if the microspheres are removed at 30 d (F(30 d) = 7.19).

Delivery and removal approaches

In the initial approach, it is likely that the microspheres will be directed into the tumor vasculature using a catheter. Image-guided radiation therapy [20,31] could be utilized to facilitate guiding the catheter to specifically target the tumor vasculature.

Accomplishing preferential blood vessel attachment requires

Table 4: ^{222}Rn and Its Daughters[a,b,c].

Nuclide	$T_{1/2}$	Radiation Type / Energy (MeV)		
		Alpha	Beta[d]	Gamma
^{222}Rn	3.8235 d	5.4895	---	0.510 (w)
^{218}Po	3.10 min	6.0024	(w)	0.510
^{214}Pb	27 min	---	0.67 0.73	0.3519 0.2952 0.2420
^{214}Bi	19.9 min	5.450 (w) 5.513	3.27 1.54 1.51	0.6093 1.1203 1.7645
^{214}Po	163.7 μs	7.6869	---	0.799 (w)
^{210}Pb	22.3 y	3.72 (vw)	0.017 0.061	0.0465
^{210}Bi	5.01 d	4.648 (vw) 4.687	1.162	0.305 (vw) 0.266
^{210}Po	138.38 d	5.3044	---	0.8031 (vw)
^{206}Pb	Stable	--	---	---

[a]Baum et al. [30].
[b]Weak (w) transition with a yield < 1%.
[c]Very weak (vw) transition with a yield < 10^{-3}%.
[d]Maximum beta or positron energy.

significant development. For example, the microsphere design effort will evaluate a variety of chemical and physical approaches (e.g., electric charge, heat, pH, and electromagnetic fields) to facilitate the preferential attachment of the microsphere to the tumor's vascular wall. The specific microsphere design characteristics that require experimental investigation include material composition, electric charge and its spatial distribution, physical size and shape, and dielectric and diamagnetic properties. Final microsphere design may be enhanced using activating agents, which could include the use of lasers, heat, and a spectrum of electromagnetic radiation. Both the microsphere design and activating agents require extensive verification efforts.

The removal approach would in principle be accomplished by reversing the attachment protocol. For example, placement and subsequent removal could be achieved by embedding a magnetic material within the microsphere. The magnetic particles facilitate placement in the desired location using an active, localized magnetic field. Eliminating the magnetic field would facilitate microsphere removal. The protocol for microsphere implantation and removal require additional research and development.

Half-life issues

An additional issue associated with ^{210}Po microspheres is their physical half-life. ^{210}Po and ^{90}Y are very different in terms of their physical half-lives (T_p) which must be addressed before the proposed approach can be advanced as a viable treatment protocol. ^{210}Po has a physical half-life of 138 days while ^{90}Y's half-life is only 2.7 days. The treatment delivery method used for ^{90}Y (liver cancer for example) may not work for ^{210}Po if the microsphere construction does not limit the biological half-life of the device. For example, some ^{90}Y microspheres may flow with blood into the lung and remain in healthy tissue. For a relatively short physical half-life material like ^{90}Y, this does not produce a significant concern. However, the longer physical half-life of ^{210}Po would produce a larger residual lung dose that could create a significant biological detriment. This concern is alleviated if the ^{210}Po microspheres are constructed of a material that has a short-biological half-life in the lung.

The capability to construct microspheres with a short lung retention time is a necessary design requirement for the final ^{210}Po development effort. For example, the microspheres will be constructed of a material with ICRP 30 [32] Class D lung retention characteristics. As defined in ICRP 30, Class D material has a biological half-life in the lung that is less than 10 days. Part of the development effort will be the construction of a microsphere with a short biological retention time in the lung. Since the effective half-life (T_e) of a radionuclide depends on its biological and physical half-lives, a longer physical half-life is not a limiting factor if the biological half-life (T_b) is short. The effective half-life of the ^{210}Po microsphere in the lung is given by the standard relationship [33]:

$$T_e = \frac{T_p\ T_b}{T_p + T_b} \qquad (9)$$

The ^{210}Po microsphere effective half-life in the lung for a Class D material with 2 and 10 day biological half-lives is 1.97 and 9.32 days, respectively. A microsphere design requirement for an ICRP Class D level biological half-life in the lung eliminates the concern associated with the longer ^{210}Po physical half-life.

^{210}Po Toxicity and patient safety

^{210}Po has a specific activity of 1.7 x 10^{14} Bq/g and its inhalation (ingestion) effective dose coefficient is 3.0 x 10^{-6} Sv/Bq (2.4 x 10^{-7} Sv/Bq) [34]. The microsphere intake pathway caused by leaching has not been evaluated, but its effective dose coefficient is probably in the range of the established conventional intake pathway values, which is approximately 10^{-6} Sv/Bq. For the proposed base case microsphere of 0.3 Bq, complete ^{210}Po leaching from a single microsphere would lead to an effective dose of about 0.3 μSv. Since the number of microspheres would be utilized in a therapy protocol, the effective dose from complete leakage is limited only if the microspheres have good retention characteristics. However, the final microsphere design should have good ^{210}Po retention characteristics. With good ^{210}Po retention characteristics, the toxicity hazard to the patient is not significant. For example, if 10^6 0.3 Bq microspheres were administered with a ^{210}Po retention of 90%, the patient 50 year effective dose commitment is only 30 mSv.

Conclusion

Microspheres loaded with alpha emitting radionuclides preferentially deposit dose in the target tissues while minimizing the dose delivered to healthy tissue. However, these radionuclides must have weak beta and gamma emissions to selectively deposit absorbed dose in the target vasculature. This selective dose deposition minimizes stray dose and limits the side effects that often accompany radiotherapy procedures. The microsphere approach can be realized in the near-term, but additional research and development is required to develop the techniques proposed in this paper into a practical radiotherapy protocol.

Acknowledgment

The author thanks Dr. M. L. Raghavan of Iowa State University for assistance in obtaining relevant vascular data. Dr. Paul Rittmann and Joe Shonka provided copies of the ISO-PC and ISOSHLD-II codes, respectively. Finally, useful information regarding ^{90}Y microsphere administration and associated operational considerations were provided by GE Healthcare (J. L. Herner) and the University of Wisconsin – Madison (V. Goretske).

References

1. Bevelacqua JJ. Systematics of heavy ion radiotherapy. Radiation Protection Management. 2005; 22: 4-13.

2. Bevelacqua JJ. Feasibility of using internal radiation-generating devices in radiotherapy. Health Phys. 2010; 98: 614–620.

3. Bevelacqua JJ. Angular absorbed dose dependence of internal radiation-generating devices in radiotherapy. Health Phys. 2012; 102: 2–7.

4. Bevelacqua JJ. Tumor vascular disruption using various radiation types. Peer J. 2014; 2: e320.

5. Bevelacqua JJ. ^{210}Po microsphere radiological design for tumor vascular disruption. Peer J. 2015; 3: e1143.

6. Bevelacqua JJ. Health Physics: Radiation-Generating Devices, Characteristics, and Hazards. Weinheim: Wiley-VCH. 2016; 800.

7. Martinez AA, Gonzalez JA, Chung AK, Kestin LL, Balasubramaniam M, Diokno AC, et al. A comparison of external beam radiation therapy versus radical prostatectomy for patients with low risk prostate carcinoma diagnosed, staged and treated at a single institution. Cancer. 2000; 88: 425-432.

8. NCRP Report No. 170. Second primary cancers and cardiovascular disease after radiation therapy. 2012; Bethesda: NCRP Publications.

9. Folkman J. Tumor angiogenesis: therapeutic implications. N Eng J Med. 1971; 285: 1182–1186.

10. Burke PA, DeNardo SJ. Antiangiogenic agents and their promising potential in combined therapy. Crit Rev Oncol Hematol. 2001; 39: 155–171.

11. Carmeliet P, Jain RK. Angiogenesis in cancer and other diseases. Nature. 2000; 407: 249–257.

12. Rajput MS, Agrawal P. Microspheres in cancer therapy. Indan J Cancer. 2010; 47: 458–468.

13. Kennedy AS, Salem R. Comparison of two ^{90}Yttrium microsphere agents for hepatic artery brachytherapy. In: Proceedings of the 14th International Congress on Anti-cancer Treatment; 5-7 February 2013; ICACT, Paris: International Congress on Anti-Cancer Treatment. 2013; 1–156.

14. Carr BI. Hepatic arterial ^{90}Y glass microspheres (Therasphere) for unresectable hepatocellular carcinoma: interim safety and survival data on 65 patients. Liver Transplantation. 2004; 10: S107–S110.

15. Murthy R, Nunez R, Szklaruk F, Erwin W, Madoff DC, Gupta S, et al. Yttrium-90 microsphere therapy for hepatic malignancy: devices, indications, technical considerations, and potential complications. Radiographics. 2005; 25: S41–S55.

16. Kennedy A, Nag S, Salem R, Murthy R, McEwan AJ, Nutting C, et al. Recommendations for radioembolization of hepatic malignancies using Yttrium-90 microsphere brachytherapy: a consensus panel report from the radioembolization brachytherapy oncology consortium. Int J Radiat Oncol Biol Phys. 2007; 68: 13–23.

17. Chaudhury PK, Hassanain M, Bouteaud JM, Alcindor T, Nudo CG, Valenti D, et al. Complete response of heptocellular carcinoma with sorafenib and ^{90}Y radioembolization. Current Oncology. 2010; 17: 67–69.

18. Dezarn WA, Cessna JT, DeWerd LA, Feng W, Gates VL, Halama J, et al. Recommendations of the American Association of Physicists in Medicine on dosimetry, imaging, and quality assurance procedures for ^{90}Y microsphere brachytherapy in the treatment of hepatic malignancies. Medical Physics. 2011; 38: 4824–4845.

19. Lau WY, Lai EC, Leung TW. Current role of selective internal irradiation with yttrium-90 microspheres in the management of hepatocellular carcinoma: a systematic review. Int J Radiat Oncol Biol Phys. 2011; 81: 460–467.

20. Lee IK, Seong J. The optimal selection of radiotherapy treatment for hepatocellular carcinoma. Gut and Liver. 2012; 6: 139–148.

21. Amor-Coarasa A, Milera A, Carvajal D, Gulec S, McGoron AJ. ^{90}Y-DOTA-CHS microspheres for live radiomicrosphere therapy: preliminary *in vivo* lung radiochemical stability studies. J Radiother. 2014; 2014: 1–6.

22. Holzscheiter M, Bassler N, Agazaryan N, Beyer G, Blackmore E, DeMarco J, et al. The biological effectiveness of antiproton irradiation. Radiother Oncol J. 2006; 81: 233–242.

23. Bittner M, Grosu A, Wiedenmann N, Wilkens JJ. A systematic review of antiproton radiotherapy. Frontiers in Physics. 2013; 1: 1-8.

24. Barrett KE, Barman SM, Boitano S, Brooks H. Ganong's review of medical physiology. 24th edition. New York: McGraw-Hill Medical. 2012; 752.

25. Kraft G. Tumor therapy with heavy charged particles. Progress in Particle and Nuclear Physics. 2000; 45: S473-S544.

26. Bethe H. Zur theorie des durchgangs schneller korpuskularstrahlung durch materie. Annalen der Physik. 1930; 5: 325–400.

27. Shen WQ, Wang B, Feng J, Zhan WL, Zhu YT, Feng EP. Total reaction cross section for heavy-ion collisions and its relation to the neutron excess degree of freedom. Nuclear Physics A. 1989; 491: 130–146.

28. Rittmann PD. ISO-PC version 2.2-user's guide. Richland: Fluor Government Group. 2004.

29. IAEA. Relative biological effectiveness in ion beam therapy, International Atomic Energy Agency, IAEA Technical Reports Series, No. 461. Vienna: IAEA. 2008.

30. Baum EM, Ernesti MC, Knox HD, Miller TR, Watson AM. Nuclides and isotopes chart of the nuclides. 17th edition. Schnectady: Knowles Atomic Power Laboratory. 2010.

31. National Cancer Action Team. National radiotherapy implementation group report. Image guided radiotherapy (IGRT): Guidance for implementation and use. London: NCAT. 2012.

32. ICRP Publication 30. Limits for intakes of radionuclides by workers. Oxford: Pergamon. 1979.

33. Bevelacqua JJ. Basic health physics: problems and solutions. 2nd edition. Weinheim: Wiley-VCH. 2010; 743.

34. ICRP Publication 119. Compendium of dose coefficients based on ICRP publication 60. Amsterdam: Elsevier. 2012.